



LETTER

Dynamics of breather waves and higher-order rogue waves in a coupled nonlinear Schrödinger equation

To cite this article: Wei-Qi Peng *et al* 2018 *EPL* **123** 50005

View the [article online](#) for updates and enhancements.

You may also like

- [Soliton molecules, breather molecules and stability analysis of the three-coupled nonlinear Schrödinger equation](#)
Zuoxin Xiong and Bo Ren
- [Provable bounds for the Korteweg–de Vries reduction in multi-component nonlinear Schrödinger equation](#)
Swetlana Swarup, Vishal Vasan and Manas Kulkarni
- [Binary Darboux transformation and vector-soliton-pair interactions with the negatively coherent coupling in a weakly birefringent fiber](#)
Chen-Rong Zhang, Bo Tian, Yan Sun *et al.*

Dynamics of breather waves and higher-order rogue waves in a coupled nonlinear Schrödinger equation

WEI-QI PENG, SHOU-FU TIAN^(a) and TIAN-TIAN ZHANG

School of Mathematics and Institute of Mathematical Physics, China University of Mining and Technology Xuzhou 221116, PRC

received 18 June 2018; accepted in final form 11 September 2018
published online 5 October 2018

PACS 02.30.Ik – Integrable systems

PACS 05.45.Yv – Solitons

PACS 52.35.Mw – Nonlinear phenomena: waves, wave propagation, and other interactions
(including parametric effects, mode coupling, ponderomotive effects, etc.)

Abstract – We consider a coupled nonlinear Schrödinger (NLS) equation, which can be reduced to the generalized NLS equation by constituting a certain constraint. We first construct a generalized Darboux transformation (DT) for the coupled NLS equation. Then, by using the resulting DT, we analyse the solutions with vanishing boundary condition and non-vanishing boundary condition, respectively, including positon wave, breather wave and higher-order rogue wave solutions for the coupled NLS equation. Moreover, in order to better understand the dynamic behavior, the characteristics of these solutions are discussed through some diverting graphics under different parameters choices.

Copyright © EPLA, 2018

Introduction. – Rogue waves (RWs), also known as killer waves, extreme waves, giant waves, have been gradually extended to diverse fields, such as shallow waters and deep ocean, nonlinear optics, Bose-Einstein (BE) condensates, finance, etc. [1–8]. Especially, RWs are constructed with relation to supercontinuum generation (SCG) in photonic crystal fibers, which can motivate the corresponding researches for RWs in some physical models. RWs, appearing abruptly and disappearing without any trace, primarily cover the prominent characteristics of high peak and being rationally localized. There are some main propelling methods in studying RWs, containing Wronskian technique, Bäcklund transformation, Darboux transformation (DT) method and the bilinear method [9–17]. Generally, the nonlinear Schrödinger (NLS) equation is regarded as a common model to describe RWs [18]. The NLS equation arises from different fields, such as nonlinear optics, deep water waves and plasma physics [19–24]. In recent years, the generalized formalizations of the NLS equation involving additional terms and derivatives have been studied extensively in order to reflect the contributions of higher-order nonlinear effects which cannot be ignored in optical fibers [25]. One example of the above consideration is a

generalized NLS introduced in ref. [26], namely,

$$iu_t + u_{xx} - 2\delta|u|^2u + 4\beta^2|u|^4u + 4i\delta\beta(|u|^2)_xu = 0, \quad (1)$$

where $u(x, t)$ is a complex valued function of the real variables x and t , β is a real constant, and $\delta = \pm 1$. When $\delta = -1$, eq. (1) reduces to the Kundu-Eckhaus (KE) equation which has a Lax representation and Hamiltonian structure. Plentiful results have been presented by a series of methods [27–32].

In this paper, we mainly focus on a coupled NLS equation

$$\begin{aligned} iu_t + u_{xx} - 2u^2v + 4\beta^2u^3v^2 + 4i\beta(uv)_xu &= 0, \\ iv_t - v_{xx} + 2uv^2 - 4\beta^2u^2v^3 + 4i\beta(uv)_xv &= 0, \end{aligned} \quad (2)$$

through the generalized Darboux transformation. When $u^* = \delta v$, eq. (2) reduces to the above eq. (1), $*$ denotes the complex conjugation. The soliton solutions have been derived based on the Darboux transformation in [33].

To the best of our knowledge, the positon waves, breather waves and higher-order rogue waves of (2) have not been investigated by using the method of the generalized Darboux transformation. In this work, the generalized Darboux transformation for eq. (2) is briefly introduced to find these solutions.

^(a)E-mail: shoufu2006@126.com, sftian@cumt.edu.cn (corresponding author)

Generalized Darboux transformation. – Next, we construct a generalized Darboux transformation for the coupled NLS equation (2) whose Lax pair has been given in [33]. According to the variable transformation

$$u = qe^{-2i\beta \int q r dx}, \quad v = re^{2i\beta \int q r dx}, \quad (3)$$

the spectral problem for (2) can be turned into the following standard AKNS spectral problem, given by

$$\Phi_x = \mathcal{U}\Phi, \quad \Phi_t = \mathcal{V}\Phi = (\mathcal{V}_2\lambda^2 + \mathcal{V}_1\lambda + \mathcal{V}_0)\Phi \quad (4)$$

with

$$\mathcal{U} = \begin{pmatrix} -i\lambda & q \\ r & i\lambda \end{pmatrix}, \quad \mathcal{V}_2 = \begin{pmatrix} -2i & 0 \\ 0 & 2i \end{pmatrix}, \quad \mathcal{V}_1 = \begin{pmatrix} 0 & 2q \\ 2r & 0 \end{pmatrix}, \quad (5)$$

$$\mathcal{V}_0 = \begin{pmatrix} v_{11} & iq_x \\ -ir_x & -v_{11} \end{pmatrix}, \quad v_{11} = \beta(q_x r - q r_x) - iq r + i\beta \int (qr)_t dx, \quad (6)$$

where $\Phi(x, t, \lambda) = (\phi, \varphi)^T$ is the new eigenfunction, and $q = q(x, t)$ and $r = r(x, t)$ are two new potentials.

Theorem 1. *Supposing $\Phi_1(\lambda_1 + \epsilon)$ is a basic solution to the Lax pair equations (4) related to $\{q = q[0], r = r[0]\}$ and $\lambda = \lambda_1 + \epsilon$, of which ϵ is an infinitesimal parameter, and expanding Φ_1 at $\epsilon = 0$ by higher-order Taylor expansion, we have*

$$\Phi_1 = \Phi_1^{[0]} + \Phi_1^{[1]}\epsilon + \Phi_1^{[2]}\epsilon^2 + \dots + \Phi_1^{[n]}\epsilon^n + \dots, \quad (7)$$

where

$$\Phi_1^{[k]} = \left(\phi_1^{[k]}, \varphi_1^{[k]} \right)^T = \frac{1}{k!} \frac{\partial^k \Phi_1}{\partial \epsilon^k} \Big|_{\epsilon=0}, \quad k = 0, 1, 2, \dots \quad (8)$$

Thus, $\{u[n], v[n]\}$ presented by the following formulae are new solutions of the CNLS equation (2) with $\delta = -1$:

$$u[n] = q[n]e^{-2i\beta \int q[n]r[n]dx}, \quad v[n] = r[n]e^{2i\beta \int q[n]r[n]dx}, \quad (9)$$

and

$$q[n] = q - 2i(\lambda_1 - \lambda_1^*) \sum_{j=0}^{n-1} \frac{\phi_1[j]\varphi_1[j]^*}{|\phi_1[j]|^2 + |\varphi_1[j]|^2}, \quad (10)$$

$$r[n] = r + 2i(\lambda_1 - \lambda_1^*) \sum_{j=0}^{n-1} \frac{\phi_1[j]^*\varphi_1[j]}{|\phi_1[j]|^2 + |\varphi_1[j]|^2},$$

where

$$\Phi_1^{[0]} = \Phi_1[0], \quad \Phi_1[j] = (\phi_1[j], \varphi_1[j])^T,$$

$$\Phi_1[j] = \Phi_1^{[0]} + \sum_{k=1}^j T_1[k]\Phi_1^{[1]} + \sum_{k=1}^j \sum_{s=1}^{k-1} T_1[k]T_1[s]\Phi_1^{[2]} + \dots + T_1[j]T_1[j-1] \dots T_1[1]\Phi_1^{[j]}, \quad j = 0, 1, 2, \dots, \quad (11)$$

$$T_1[j] = \lambda I - H[j-1]\Lambda_j H[j-1]^{-1}, \quad I = \begin{pmatrix} 1 & 0 \\ 0 & 1 \end{pmatrix}, \quad (12)$$

$$H[j-1] = \begin{pmatrix} \phi_1[j-1] & -\varphi_1[j-1]^* \\ \varphi_1[j-1] & \phi_1[j-1]^* \end{pmatrix}, \quad \Lambda_j = \begin{pmatrix} \lambda_1 & 0 \\ 0 & \lambda_1^* \end{pmatrix}. \quad (13)$$

It is trivial to confirm $q^* = -r$, thus N steps of the Darboux transformation meet $q[n]^* = -r[n]$. Apparently, we have $u^* = -v$ and $u[n]^* = -v[n]$.

Solutions with vanishing boundary condition. –

Next, we start from a zero seed solution to construct positon solutions by employing Theorem 1. Let $u = 0$, on the basis of the transformation (3), we obtain $q = 0$ which can be used to generate an essential solution to the Lax pair equations (4). Inspired by the physical importance of DT theory in multi-rational solutions [34,35], we take $\lambda = \xi + i\eta$, then the solutions of the Lax pair equations (4) with eigenvalues λ are solved as

$$\Phi_1 = \begin{pmatrix} e^{-i((\xi+i\eta)x+2(\xi+i\eta)^2t+\sum_{k=1}^n p_k \epsilon^{2k})} \\ e^{i((\xi+i\eta)x+2(\xi+i\eta)^2t+\sum_{k=1}^n p_k \epsilon^{2k})} \end{pmatrix}. \quad (14)$$

Taking $\eta = 1 - i\epsilon^2$ and expanding the vector function $\Phi_1(\epsilon)$ at $\epsilon = 0$, we have

$$\Phi_1(\epsilon) = \Phi_1^{[0]} + \Phi_1^{[1]}\epsilon^2 + \Phi_1^{[2]}\epsilon^4 + \dots, \quad (15)$$

where $\Phi_1^{[j]} = (\phi_1^{[j]}, \varphi_1^{[j]})^T$, ($j = 0, 1, 2, 3, \dots$), and $p_k = m_k + s_k i$. Letting $\lambda = \lambda_1 = \xi + i$, and using Theorem 1, we obtain the one-positon wave solutions by taking $n = 2$

$$q[2]_{Pws} = \frac{4G}{F} \exp(i(-2\xi x + 4t - 4\xi^2 t)), \quad (16)$$

where

$$G = (8it + 2s_1 i + 1)[\cosh(6x + 24\xi t) + 3 \cosh(2x + 8\xi t)] - (2x + 8\xi t + 2m_1)[\sinh(6x + 24\xi t) + \sinh(2x + 8\xi t)],$$

$$F = \cosh(2x + 8\xi t)[(16(4\xi t + x + m_1)^2 + 16(4t + s_1)^2 + 3) \cosh(2x + 8\xi t) + \cosh(6x + 24\xi t)]. \quad (17)$$

Naturally, the one-positon solutions for (2) admit the following expression:

$$u[2]_{Pws} = q[2]_{Pws} e^{-2i\beta \int q[2]_{Pws} r[2]_{Pws} dx}, \quad (18)$$

where $\int q[2]_{Pws} r[2]_{Pws} dx = -\frac{8H}{D}$ with

$$H = (8(4\xi t + x + m_1)^2 + 8(4t + s_1)^2 + 16\xi t + 4m_1 + 4x + 1) \exp(-4x - 16\xi t) + 1,$$

$$D = (16(4\xi t + x + m_1)^2 + 16(4t + s_1)^2 + 2) \exp(-4x - 16\xi t) + \exp(-8x - 32\xi t) + 1. \quad (19)$$

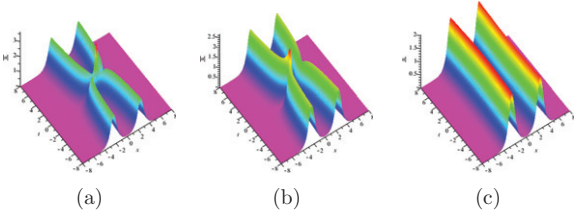


Fig. 1: (Color online) Profiles of the one-positon solutions (18) with the parameters $\xi = 0, s_1 = 0$ and (a) $m_1 = 0$, (b) $m_1 = 2$, (c) $m_1 = 30$.

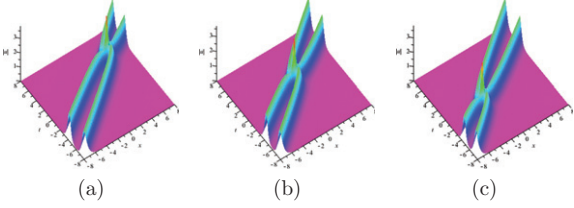


Fig. 2: (Color online) Profiles of the one-positon solutions (18) with the parameters $\xi = -\frac{1}{3}, m_1 = 0$ and (a) $s_1 = -10$, (b) $s_1 = 0$, (c) $s_1 = 10$.

In fact, the one-positon wave solutions (18) represent the interaction of two-soliton solutions, and the high peak comes from the interaction of two solitons under the degeneration of the associated eigenvalues. The corresponding dynamic characteristics of the solutions are discussed in figs. 1 and 2. Figure 1 shows the process of evolution for different selections of parameter $m_1 = 0, m_1 = 2, m_1 = 30$, respectively. we can easily find that the high peak is swallowed by the two solitons as m goes up. The high peak appears at $m_1 = 0$, and then the one-positon wave solutions (18) reduce to the two-soliton waves. As shown in fig. 2, we find that parameter s_1 affects the phase of the high peak. In addition, by comparing fig. 1(a) with fig. 1(b), we understand that the distance between two solitons depends on the parameter ξ .

Solutions with a non-vanishing boundary condition. – Next, we discuss the solutions from a non-trivial seed. Without loss of generality, starting with $u[0] = \exp(i\theta), \theta = (ax + bt), b = 4\beta^2 - a^2 + 2, a \in \mathbb{R}$, we shall present the breather solutions and higher-order rogue wave solutions of the coupled nonlinear Schrödinger equation. Based on the transformation (9), we have the non-trivial seed for the Lax pair equations (4), reading as $q[0] = \exp(ax - 2\beta x + bt)$. Then the new eigenfunctions corresponding to $\lambda = ic + \beta - \frac{a}{2}$ can be provided by

$$\Phi_1 = \begin{pmatrix} \omega_1 \exp(\varpi + \frac{i}{2}\theta) - \omega_2 \exp(-\varpi + \frac{i}{2}\theta) \\ \omega_1 \exp(-\varpi - \frac{i}{2}\theta) - \omega_2 \exp(\varpi - \frac{i}{2}\theta) \end{pmatrix}, \quad (20)$$

with

$$\omega_1 = \frac{(c - \sqrt{c^2 - 1})^{\frac{1}{2}}}{\sqrt{c^2 - 1}}, \quad \omega_2 = \frac{(c + \sqrt{c^2 - 1})^{\frac{1}{2}}}{\sqrt{c^2 - 1}},$$

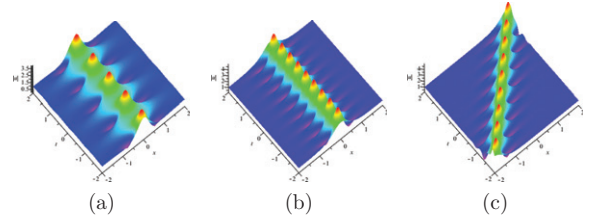


Fig. 3: (Color online) Profiles of the first-order breather waves for (23) with the parameters (a) $a = 0, \beta = 0, c = \frac{3}{2}$, (b) $a = 0, \beta = 0, c = 2$, (c) $a = \frac{1}{2}, \beta = 0, c = 2$.

$$\varpi = -\sqrt{c^2 - 1} \left(x + 4\beta t + 2ict - 2at + \sum_{k=1}^n p_k \varepsilon^{2k} \right). \quad (21)$$

First-order breather and rogue wave solutions. Next, we shall analyse the solutions with a non-vanishing boundary condition for the case of $p_k = 0$. On account of $\Phi_1^{[0]} = \Phi_1[0]$, we can derive first-order breather waves,

$$q[1]_{Bws} = \frac{\widetilde{G}_1}{\widetilde{F}_1} \exp(i(ax - 2\beta x + 4\beta^2 t - a^2 t + 2t)), \quad (22)$$

where

$$\begin{aligned} \widetilde{G}_1 &= c \cosh [2\sqrt{c^2 - 1}(2at - 4\beta t - x)] \\ &\quad + (1 - 2c^2) \cos(4c\sqrt{c^2 - 1}t) \\ &\quad - 2c\sqrt{c^2 - 1}i \sin(4c\sqrt{c^2 - 1}t), \\ \widetilde{F}_1 &= \cos(4c\sqrt{c^2 - 1}t) \\ &\quad - c \cosh[2\sqrt{c^2 - 1}(2at - 4\beta t - x)]. \end{aligned}$$

Naturally, the first-order breather wave solutions for (2) admit the expression

$$u[1]_{Bws} = q[1]_{Bws} e^{-2i\beta \int q[1]_{Bws} r[1]_{Bws} dx}$$

with $r[1]_{Bws} = -q[1]_{Bws}^*$.

In fig. 3, the first-order breather wave solutions are shown which progress periodically along a certain straight line. As depicted in figs. 3(a) and (b), the waves, called KM breather waves, are periodic in time and localized in space for fixed $a = \beta = 0$. Moreover, the increase of parameter c leads to the decrease of the KM breather waves period. But when a turns into $\frac{1}{2}$, the breather waves evolve with a certain angle with the x -axis and t -axis.

We have known that the breather waves are a type of periodic wave. Obviously, $\frac{2\pi}{\sqrt{c^2 - 1}}$ denotes the period of eq. (22). When the period $\frac{2\pi}{\sqrt{c^2 - 1}}$ tends to infinity, the breather waves can transform into the rogue waves. Therefore, we take $c \rightarrow 1$, the first-order rogue waves of (2) can be written as

$$q[1]_{Rws} = \left(1 - 2\frac{G_1}{F_1} \right) \exp(i(ax - 2\beta x + 4\beta^2 t - a^2 t + 2t)), \quad (23)$$

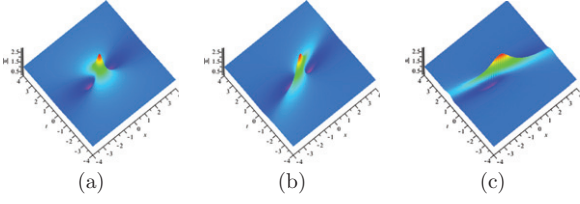


Fig. 4: (Color online) Profiles of the first-order rogue wave solutions (24) with the parameters (a) $a = 0, \beta = 0$, (b) $a = \frac{2}{3}, \beta = 0$, (c) $a = 0, \beta = \frac{4}{5}$.

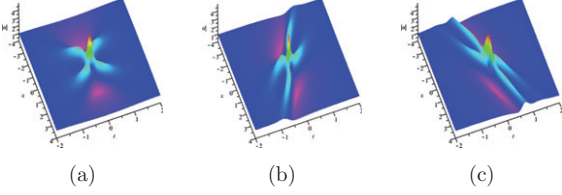


Fig. 5: (Color online) Profiles of the second-order rogue wave solutions (24) with the parameters $m_1 = s_1 = 0$ (a) $a = 0, \beta = 0$, (b) $a = 0, \beta = \frac{2}{3}$, (c) $a = 2, \beta = 0$.

where

$$\begin{aligned} G_1 &= (4at - 8\beta t - 2x)^2 - (4it + 1)^2, \\ F_1 &= 16(at - 2\beta t)(at - 2\beta t - x) + 16t^2 + 4x^2 + 1. \end{aligned} \quad (24)$$

Naturally, the first-order rogue wave solutions for (2) admit the following expression:

$$u[1]_{Rws} = q[1]_{Rws} e^{-2i\beta \int q[1]_{Rws} r[1]_{Rws} dx}, \quad (25)$$

where $\int q[1]_{Rws} r[1]_{Rws} dx = -\frac{H_1}{D_1}$ with

$$\begin{aligned} H_1 &= 4x^3 + 16(2\beta - a)(x^2 + 1)t \\ &\quad + 16((2\beta - a)^2 + 1)t^2x + 9x, \\ D_1 &= 4x^2 + (32\beta - 16a)tx \\ &\quad + 16(4\beta^2 - 4a\beta + a^2 + 1)t^2 + 1. \end{aligned} \quad (26)$$

It is easily calculated that the maximum amplitude of $|u[1]_{Rws}|$ is equal to 3 times that of the background plane wave. Three graphics are displayed in fig. 4 through different selections of parameters a and β . The fact that a and β affect the phase of rogue waves can be attested by fig. 4. In addition, as β increases, the angle between the ridge of the rogue waves and the x -axis becomes larger. Similarly, the change of a can also result in the corresponding angle change.

Higher-order rogue wave solutions. In the above method, the first-order rogue wave solutions have also been obtained by an advisable limit from the breather solutions. However, the method is hard for calculating the higher-order rogue waves. Here, we discuss the higher-order rogue waves in terms of the generalized Darboux transformation (see Theorem 1). Analogously, we take $c = 1 - i\varepsilon^2$, and carry out the Taylor expansion as (15). It is not difficult to verify that the first-order waves obtained by Theorem 1 are completely consistent with the

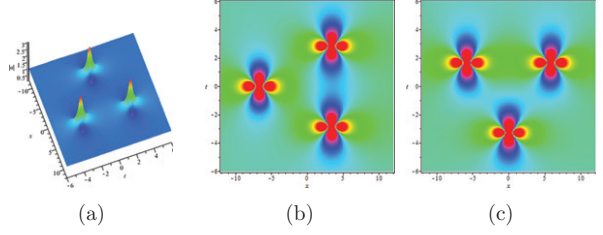


Fig. 6: (Color online) Three-dimensional plots and density plots of the second-order rogue wave solutions (24) with the parameters: (a) $a = 0, \beta = 0, m_1 = 0, s_1 = 200$, (b) $a = 0, \beta = 0, m_1 = 0, s_1 = 200$, (c) $a = 0, \beta = 0, m_1 = 200, s_1 = 0$.

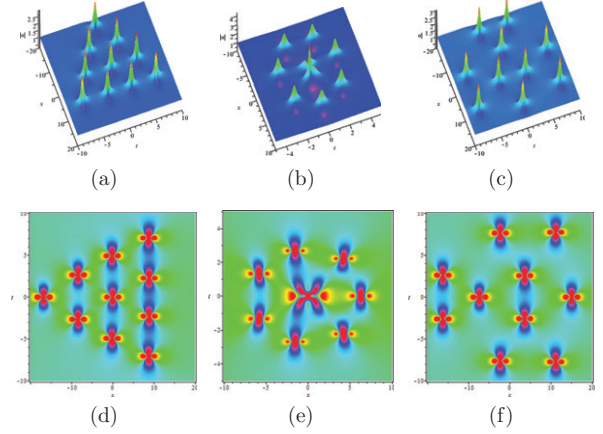


Fig. 7: (Color online) Three-dimensional plots and density plots of the fourth-order rogue wave solutions for eq. (2) with the parameters: $a = 0, \beta = 0, m_1 = 0, m_2 = 0, s_2 = 0, m_3 = 0$, ((a), (d)) $s_1 = 200, s_3 = 0$, ((b), (e)) $s_1 = 0, s_3 = 2000$, ((c), (f)) $s_1 = 200, s_3 = 2000000$.

above first-order waves (23). Therefore, we omit the case of $n = 1$, and take $n = 2$ to derive the explicit form of second-order rogue waves, constructed by

$$q[2]_{Rws} = \frac{G_2}{F_2} \exp(i(ax - 2\beta x + 4\beta^2 t - a^2 t + 2t)), \quad (27)$$

where G_2 and F_2 are six binary polynomials in x and t , which are presented in the appendix. Using the transformation in (9), we obtain the second-order rogue wave solutions for (2) $u[2]_{Rws} = q[2]_{Rws} e^{-2i\beta \int q[2]_{Rws} r[2]_{Rws} dx}$ with $r[2]_{Rws} = -q[2]_{Rws}^*$.

As shown in fig. 5, for fixed parameters $m_1 = s_1 = 0$, the second-order rogue waves have a single peak with two ridges of the rogue waves presented clearly in fig. 5(a). But with parameters a, β changed, the intersecting angle between two ridges of the rogue waves makes a difference, which can be observed in figs. 5(b) and (c). From fig. 6, for fixed parameters $a = \beta = 0$, the second-order rogue waves in fig. 5 separate into three peaks as m_1, s_1 are given a big enough value. Here, when $m_1 = 0, s_1 = 200$, the three peaks are symmetric about the straight line $t = 0$ in the (x, t) -plane. When $m_1 = 200, s_1 = 0$, the three peaks are symmetric about the straight line $x = 0$ in the (x, t) -plane. This phenomenon is easily confirmed by figs. 6(b) and (c).

In general, it is not hard to see that the higher-order rogue wave solutions can be generated by Theorem 1. However, due to their complex expressions showing these solutions, we just display some plots of the fourth-order rogue wave here by taking $n = 4$ in the Theorem. From fig. 7, we find out that parameters m_k and s_k control the distribution of these rogue waves. Figures 7(a) and (d) present the triangular distribution including ten first-order fundamental patterns. Figures 7(b) and (e) display a ring pattern with inner second-order fundamental patterns. Figures 7(c) and (f) are the ring-triangle distribution.

Conclusions and discussions. – In this paper, we have systematically studied the coupled nonlinear Schrödinger equation, which can be reduced to the generalized NLS equation. The exact solutions are presented by the generalized Darboux transformation. The one-soliton wave solutions are obtained in the circumstance of vanishing boundary. When $u[0]$ is written as $\exp(i\theta)$, a non-vanishing boundary condition, we generate the first breather wave and higher-order rogue wave solutions, respectively. The first-order rogue wave is produced by taking the limit in the first-order breather wave. Furthermore, we consider how the related parameters impact the dynamical characteristics of these exact solutions through figs. 1–6, respectively. At last, we also show some graphic analysis of the fourth-order rogue wave in fig. 7. These results presented in this paper will make us understand well the emergence of deep-ocean waves with large amplitude and the generation of few-cycle optical pulses which are launched by high-power laser. It is hoped that our results may be helpful to enrich and illustrate some other nonlinear systems.

We express our sincere thanks to the Editor and the Referees for their valuable comments. This work was supported by the Jiangsu Province Natural Science Foundation of China under Grant No. BK20181351, the Postgraduate Research & Practice Program of Education & Teaching Reform of CUMT under Grant No. YJSJG_2018_036, the Qinglan Engineering project of Jiangsu Universities, the National Natural Science Foundation of China under Grant No. 11301527, the Fundamental Research Fund for the Central Universities under the Grant No. 2017XKQY101, and the General Financial Grant from the China Postdoctoral Science Foundation under Grant Nos. 2015M570498 and 2017T100413.

APPENDIX

In eq. (27), F_2 are G_2 are given by

$$\begin{aligned} F_2 = & 4096a^6t^6 - 49152a^5\beta t^6 + 245760a^4\beta^2t^6 \\ & - 655360a^3\beta^3t^6 + 983040a^2\beta^4t^6 - 786432a\beta^5t^6 \\ & + 262144\beta^6t^6 - 12288a^5t^5x + 122880a^4\beta t^5x \\ & - 491520a^3\beta^2t^5x + 983040a^2\beta^3t^5x - 983040a\beta^4t^5x \end{aligned}$$

$$\begin{aligned} & + 393216\beta^5t^5x + 12288a^4t^6 + 15360a^4t^4x^2 \\ & - 98304a^3\beta t^6 - 122880a^3\beta t^4x^2 + 294912a^2\beta^2t^6 \\ & + 368640a^2\beta^2t^4x^2 - 393216a\beta^3t^6 - 491520a\beta^3t^4x^2 \\ & + 196608\beta^4t^6 + 245760\beta^4t^4x^2 - 24576a^3t^5x \\ & - 10240a^3t^3x^3 + 147456a^2\beta t^5x + 61440a^2\beta t^3x^3 \\ & - 294912a\beta^2t^5x - 122880a\beta^2t^3x^3 + 196608\beta^3t^5x \\ & + 81920\beta^3t^3x^3 + 768a^4t^4 - 6144a^3\beta t^4 + 18432a^2\beta^2t^4 \\ & + 12288a^2t^6 + 18432a^2t^4x^2 + 3840a^2t^2x^4 - 24576a\beta^3t^4 \\ & - 49152a\beta t^6 - 73728a\beta t^4x^2 - 15360a\beta t^2x^4 \\ & + 12288\beta^4t^4 + 49152\beta^2t^6 + 73728\beta^2t^4x^2 + 15360\beta^2t^2x^4 \\ & - 1536a^3n_1t^3 - 1536a^3t^3x + 9216a^2\beta n_1t^3 + 9216a^2\beta t^3x \\ & - 18432a\beta^2n_1t^3 - 18432a\beta^2t^3x - 12288at^5x \\ & - 6144at^3x^3 - 768atx^5 + 12288\beta^3n_1t^3 + 12288\beta^3t^3x \\ & + 24576\beta t^5x + 12288\beta t^3x^3 + 1536\beta tx^5 - 4608a^2m_1t^3 \\ & + 2304a^2n_1t^2x - 4608a^2t^4 + 1152a^2t^2x^2 \\ & + 18432a\beta m_1t^3 - 9216a\beta n_1t^2x + 18432a\beta t^4 \\ & - 4608a\beta t^2x^2 - 18432\beta^2m_1t^3 + 9216\beta^2n_1t^2x \\ & - 18432\beta^2t^4 + 4608\beta^2t^2x^2 + 4096t^6 + 3072t^4x^2 \\ & + 768t^2x^4 + 64x^6 + 4608am_1t^2x + 4608an_1t^3 \\ & - 1152an_1tx^2 + 4608at^3x - 384atx^3 - 9216\beta m_1t^2x \\ & - 9216\beta n_1t^3 + 2304\beta n_1tx^2 - 9216\beta t^3x + 768\beta tx^3 \\ & + 432a^2t^2 - 1728a\beta t^2 + 1728\beta^2t^2 + 1536m_1t^3 \\ & - 1152m_1tx^2 - 2304n_1t^2x + 192n_1x^3 + 6912t^4 \\ & - 1152t^2x^2 + 48x^4 + 288an_1t - 432atx - 576\beta n_1t \\ & + 864\beta tx + 144m_1^2 + 864m_1t + 144n_1^2 - 144n_1x \\ & + 1584t^2 + 108x^2 + 9, \end{aligned} \tag{A.1}$$

and

$$\begin{aligned} G_2 = & 45 - 786432a\beta^5t^6 - 12288a^5t^5x + 393216\beta^5t^5x \\ & + 92160a\beta t^4 + 23040at^3x - 46080\beta t^3x - 864an_1t \\ & + 18432a^3\beta t^4 + 1728\beta n_1t - 55296a^2\beta^2t^4 + 73728a\beta^3t^4 \\ & + 4608a^3t^3x - 36864\beta^3t^3x - 13824\beta^2t^2x^2 - 3456a^2t^2x^2 \\ & + 1152atx^3 - 2304\beta tx^3 + 245760\beta^4t^4x^2 - 10240a^3t^3x^3 \\ & - 24576a^3t^5x + 4096t^6 - 9216a\beta n_1t^2x + 192n_1x^3 \\ & + 720axt - 1440\beta xt + 15360a^4t^4x^2 - 98304a^3\beta t^6 \\ & - 92160\beta^2t^4 - 9216\beta n_1t^3 + 73728\beta^2t^4x^2 + 432n_1x \\ & - 36864\beta^4t^4 + 1536\beta tx^5 + 4608an_1t^3 + 12288\beta t^3x^3 \\ & + 3840a^2t^2x^4 - 122880a^3\beta t^4x^2 + 4608am_1t^2x \\ & + 368640a^2\beta^2t^4x^2 - 491520a\beta^3t^4x^2 - 983040a\beta^4t^5x \\ & + 983040a^2\beta^2t^5x - 491520a^3\beta^2t^5x + 18432a\beta m_1t^3 \\ & + 122880a^4\beta t^5x - 15360a\beta t^2x^4 - 122880a\beta^2t^3x^3 \\ & - 73728a\beta t^4x^2 - 294912a\beta^2t^5x + 61440a^2\beta t^3x^3 \\ & - 9216\beta m_1t^2x + 147456a^2\beta t^5x + 2304a^2n_1t^2x \\ & + 9216\beta^2n_1t^2x - 2880\beta^2t^2 - 720a^2t^2 \\ & + 18432a^2t^4x^2 + 81920\beta^3t^3x^3 + 196608\beta^3t^5x \end{aligned}$$

$$\begin{aligned}
& -23040a^2t^4 - 180x^2 - 1872t^2 + 12288\beta^3n_1t^3 \\
& -27648a^2\beta t^3x + 55296a\beta^2t^3x + 2880a\beta t^2 + 24576\beta t^5x \\
& -768atx^5 - 6144at^3x^3 + 9216a^2\beta n_1t^3 - 18432a\beta^2n_1t^3 \\
& -2304a^4t^4 - 12288at^5x + 294912a^2\beta^2t^6 - 393216a\beta^3t^6 \\
& +64x^6 - 144x^4 - 1152m_1tx^2 - 4608a^2m_1t^3 \\
& -18432\beta^2m_1t^3 - 8448t^4 + 15360\beta^2t^2x^4 - 1536a^3n_1t^3 \\
& -49152a^5\beta t^6 + 245760a^4\beta^2t^6 - 655360a^3\beta^3t^6 \\
& +983040a^2\beta^4t^6 + 1536m_1t^3 + 3072t^4x^2 + 768t^2x^4 \\
& +12288a^2t^6 + 49152\beta^2t^6 - 1152an_1tx^2 + 12288a^4t^6 \\
& +196608\beta^4t^6 + 4096a^6t^6 - 288m_1t - 5760t^2x^2 \\
& +144n_1^2 + 144m_1^2 - 2304n_1t^2x + i(-12288a^4t^5 \\
& +98304a^3\beta t^5 - 294912a^2\beta^2t^5 + 393216a\beta^3t^5 \\
& -196608\beta^4t^5 + 24576a^3t^4x - 147456a^2\beta t^4x \\
& +294912a\beta^2t^4x - 196608\beta^3t^4x - 24576a^2t^5 \\
& -18432a^2t^3x^2 + 98304a\beta t^5 + 73728a\beta t^3x^2 - 98304\beta^2t^5 \\
& -73728\beta^2t^3x^2 + 24576at^4x + 6144at^2x^3 - 49152\beta t^4x \\
& -12288\beta t^2x^3 + 2304a^2m_1t^2 + 4608a^2t^3 - 9216a\beta m_1t^2 \\
& -18432a\beta t^3 + 9216\beta^2m_1t^2 + 18432\beta^2t^3 - 12288t^5 \\
& -768tx^4 - 2304am_1tx - 4608an_1t^2 - 4608at^2x \\
& +4608\beta m_1tx + 9216\beta n_1t^2 + 9216\beta t^2x - 2304m_1t^2 \\
& +576m_1x^2 + 2304n_1tx - 1536t^3 + 1152tx^2 + 144m_1 \\
& -6144t^3x^2 + 720t) - 49152a\beta t^6 + 2304\beta n_1tx^2 \\
& +13824\beta^2x^2 + 262144\beta^6t^6. \tag{A.2}
\end{aligned}$$

REFERENCES

- [1] DRAPER L., *Weather*, **21** (1966) 2.
- [2] MÜLLER P., GARRETT C. and OSBORNE A., *Oceanography*, **18** (2005) 66.
- [3] KHARIF C., PELINOVSKY E. and SLUNYAEEY A., *Rogue Waves in the Ocean, Observation, Theories and Modeling* (Springer, New York) 2009.
- [4] DUDLEY J. M., DIAS F., ERKINTALO M. and GENTY G., *Nat. Photon.*, **8** (2014) 755.
- [5] SOLLI D. R., ROPERS C., KOONATH P. and JALALI B., *Nature*, **450** (2007) 1054.
- [6] BLUDOV Y. V., KONOTOP V. V. and AKHMEDIEV N., *Phys. Rev. A*, **80** (2009) 033610.
- [7] YAN Z. Y., *Phys. Lett. A*, **375** (2011) 4274.
- [8] STENFLO L. and MARKLUND M., *J. Plasma Phys.*, **76** (2010) 293.
- [9] MA W. X. and YOU Y. C., *Am. Math. Soc.*, **357** (2005) 1753.
- [10] ZHANG D. J. and CHEN D. Y., *J. Phys. A: Gen. Math.*, **37** (2004) 851.
- [11] OHTA B. Y. and YANG J., *Proc. R. Soc. A Math. Phys. Eng. Sci.*, **468** (2012) 1716.
- [12] GUO B. L., LING L. M. and LIU Q. P., *Phys. Rev. E*, **85** (2012) 026607.
- [13] WANG X., LI Y. and CHEN Y., *Wave Motion*, **51** (2014) 1149.
- [14] HE J. S., TAO Y. S., PORSEZIAN K. and FOKAS A. S., *J. Nonlinear Math. Phys.*, **20** (2013) 407.
- [15] DAI C. Q., ZHU S. Q., WANG L. L. and ZHANG J. F., *EPL*, **92** (2010) 24005.
- [16] WANG X. B., TIAN S. F., QIN C. Y. and ZHANG T. T., *EPL*, **115** (2016) 10002; WANG X. B., TIAN S. F. and ZHANG T. T., *Proc. Am. Math. Soc.*, **146** (2018) 3353; DONG M. J., TIAN S. F., YAN X. W. and ZOU L., *Comput. Math. Appl.*, **75** (2018) 957.
- [17] FENG L. L. and ZHANG T. T., *Appl. Math. Lett.*, **78** (2018) 133; YAN X. W., TIAN S. F., DONG M. J., ZHOU L. and ZHANG T. T., *Comput. Math. Appl.*, **76** (2018) 179; QIN C. Y., TIAN S. F., WANG X. B., ZHANG T. T. and LI J., *Comput. Math. Appl.*, **75** (2018) 4221.
- [18] HE J. S., ZHANG H. R., WANG L. H., PORSEZIAN K. and FOKAS A. S., *Phys. Rev. E*, **87** (2013) 052914; WANG L. H., HE J. S., XU H., WANG J. and PORSEZIAN K., *Phys. Rev. E*, **95** (2017) 042217; WANG L. H., YANG C. H., WANG J. and HE J. S., *Phys. Lett. A*, **381** (2017) 1714.
- [19] AGRAWAL G. P., *Nonlinear Fiber Optics* (Academic Press, New York) 1995.
- [20] KIVSHAR Y. S. and AGRAWAL G. P., *Optical Solitons: From Fibers to Photonic Crystals* (Academic Press, New York) 2003.
- [21] HASEGAWA A. and TAPPERT F. D., *Appl. Math. Lett.*, **23** (1973) 142.
- [22] PORSEZIAN K. and NAKKEERAN K., *Phys. Rev. Lett.*, **76** (2001) 3955.
- [23] SHABAT A. and ZAKHAROV V., *Sov. Phys. JETP*, **34** (1972) 62.
- [24] KEDZIORA D. J., ANKIEWICZ A. and AKHMEDIEV N., *Phys. Rev. E*, **85** (2012) 066601.
- [25] XU S. W., HE J. S. and WANG L. H., *J. Phys. A*, **44** (2011) 305203; XU S. W. and HE J. S., *J. Math. Phys.*, **53** (2012) 063507; ZHANG Y. S., GUO L. J., HE J. S. and ZHOU Z. X., *Lett. Math. Phys.*, **105** (2015) 853.
- [26] KUNDU A., *J. Math. Phys.*, **25** (1984) 3433.
- [27] QIU D., HE J., ZHANG Y. and PORSEZIAN K., *Proc. R. Soc. A*, **471** (2015) 0236; YUAN F., QIU D. Q., LIU W., PORSEZIAN K. and HE J. S., *Commun. Nonlinear Sci. Numer. Simul.*, **44** (2017) 45.
- [28] WANG X., YANG B., CHEN Y. and YANG Y. Q., *Phys. Scr.*, **89** (2014) 095210.
- [29] ZHU Q., XU J. and FAN E., *Appl. Math. Lett.*, **76** (2018) 81.
- [30] ZHAO L. C., LIU C. and YANG Z. Y., *Commun. Nonlinear Sci. Numer. Simul.*, **20** (2015) 9.
- [31] DECIO LEVI and CHRISTIAN SCIMITERNA, *J. Phys. A: Math. Theor.*, **42** (2009) 465203.
- [32] XIE X. Y., TIAN B., SUN W. R. and SUN Y., *Nonlinear Dyn.*, **81** (2015) 1349.
- [33] GENG X. G. and TAM H. W., *J. Phys. Soc. Jpn.*, **68** (1999) 1508.
- [34] BARONIO F., DEGASPERIS A., CONFORTI M. and WABNITZ S., *Phys. Rev. Lett.*, **109** (2012) 044102.
- [35] BARONIO F., CONFORTI M., DEGASPERIS A. and LOMBARDO S., *Phys. Rev. Lett.*, **111** (2013) 114101.